JACS
JOURNAL OF THE AMERICAN CHEMICAL SOCIETY
pubs.acs.org/JACS
Article

Strain-Induced Quinoidal Character in a Carbon Nanoring Embedding Anthracene Units

Tomohiko Nishiuchi,* Yuta Makihara, and Takashi Kubo

Cite This: J. Am. Chem. Soc. 2025, 147, 37488−37496
Read Online
ACCESS | Metrics & More | Article Recommendations | Supporting Information

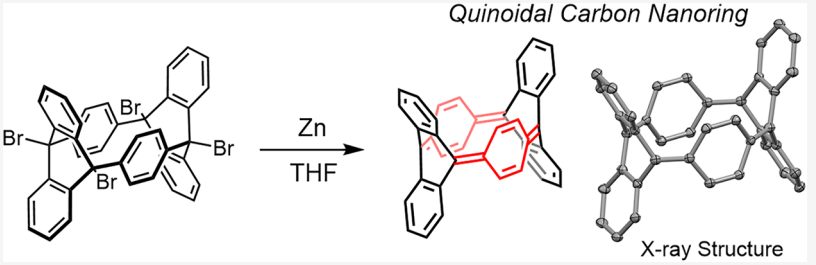

ABSTRACT: We report a carbon nanoring, [2.2]cyclo(9,10)anthrylene-paraphenylene ([2.2]CAPP), featuring alternating anthracene and phenylene units within a [4]cycloparaphenylene (CPP) framework. The molecule was synthesized via a six-step metal-free route and structurally characterized by single-crystal X-ray diffraction. The high ring strain induces significant distortion in the anthracene units, resulting in a quinoidal electronic structure with a suppressed aromaticity. Despite possessing a 16π-electron conjugation pathway, no global antiaromaticity was observed. This work demonstrates that strain engineering in carbon nanorings enables control over the aromaticity and open-shell character through rational molecular design.

INTRODUCTION

Ring- and belt-shaped aromatic hydrocarbons, such as carbon nanorings and nanobelts, have long attracted attention due to their unique π-conjugated frameworks and the resulting electronic properties predicted by computational studies.[1−7] Numerous synthetic challenges have been overcome to access these structures, significantly advancing the chemistry of carbon nanorings and nanobelts (Figure 1a).[8−46] In the case of cycloparaphenylenes (CPPs), the relationship between the ring size and electronic properties, such as the highest occupied molecular orbital-lowest unoccupied molecular orbital (HOMO−LUMO) gap, is particularly intriguing. Larger [n]CPPs (where n represents the number of phenylene rings) show properties similar to those of linear [n]-paraphenylenes (PPs), while smaller [n]CPPs exhibit narrower HOMO−LUMO gaps than their linear analogues.[47] This effect arises because the ring strain in smaller CPPs destabilizes the aromatic character of the phenylene units, leading to quinoidal contributions in the CPP framework. Computational studies indicate that larger CPPs exhibit a benzenoid character, whereas smaller ones like [3]CPP show a fully quinoidal character, reflecting strain-induced aromatic destabilization and the emergence of 1,4-biradical character localized on the phenylene units (Figure 1b).[48] This size-dependent aromaticity in CPPs provides a unique opportunity to control their electronic structures via strain engineering. Experimentally, [5]CPP has been synthesized and confirmed to adopt a benzenoid structure,[49,50] yet it exhibits interesting optical properties due to its relatively small HOMO−LUMO gap. Further reductions in ring size, such as in [4]CPP, are desirable to deepen the understanding of these size effects.[51,52] However, the synthesis of pristine [4]CPP remains elusive due to significant synthetic challenges. Notably, in 1996, Herges and co-workers synthesized "picotube", an octabenzoannulated [4]CPP derivative incorporating anthrylene units, which adopts a fully quinoidal structure with severely bent anthracene units due to steric repulsion.[53−55]

To explore the relationship between ring strain and aromaticity while mitigating steric congestion, we focused on a hybrid [4]CPP-type structure, [2.2]cyclo(9,10)anthrylene-paraphenylene ([2.2]CAPP), in which two anthrylene and two phenylene rings are alternately arranged to form a [4]CPP framework (Figure 1c). This design is expected to reduce the steric hindrance observed in a picotube while retaining significant ring strain to modulate aromaticity. Therefore, [2.2]CAPP serves as an ideal candidate for elucidating whether a benzenoid or quinoidal structure is favored.[56] Despite this potential, only several reports have described CPP derivatives incorporating 9,10-anthrylene units, likely due to synthetic

Received: July 13, 2025
Revised: October 2, 2025
Accepted: October 2, 2025
Published: October 7, 2025

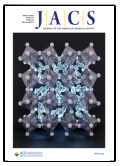

https://doi.org/10.1021/jacs.5c11812
J. Am. Chem. Soc. 2025, 147, 37488−37496

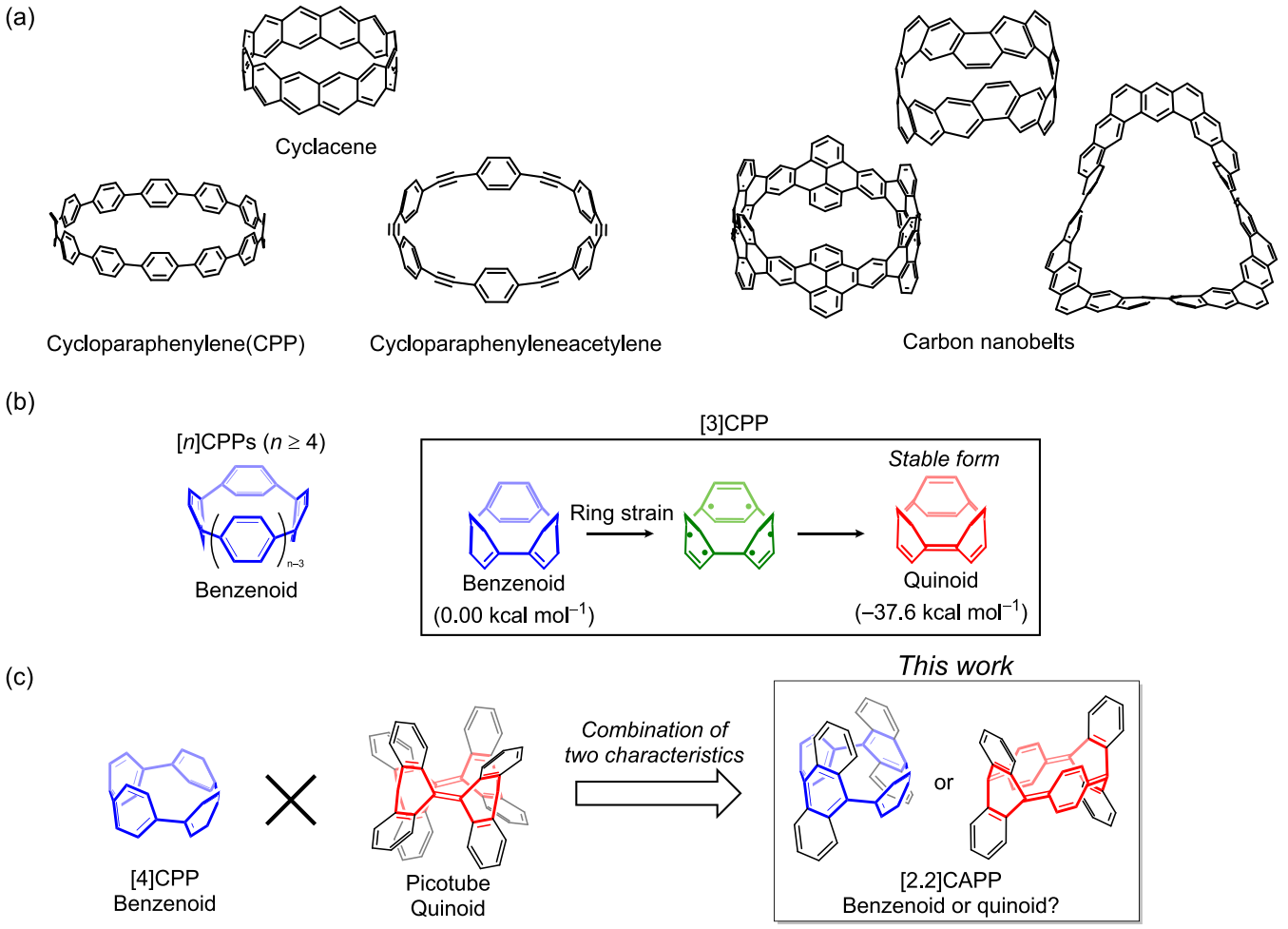

Figure 1. (a) Typical examples of carbon nanorings and nanobelt. (b) Structure of [*n*]CPPs ($n \geq 4$, left) and [3]CPP (right) with calculated relative energies of benzenoid and quinoidal forms. (c) Structures of [4]CPP, picotube, and both benzenoid and quinoidal structures of [2.2]CAPP.

Scheme 1. Synthetic Route to [2.2]CAPP (left) and X-ray Structure of Compound 1 from Two Viewpoints (right)[a]

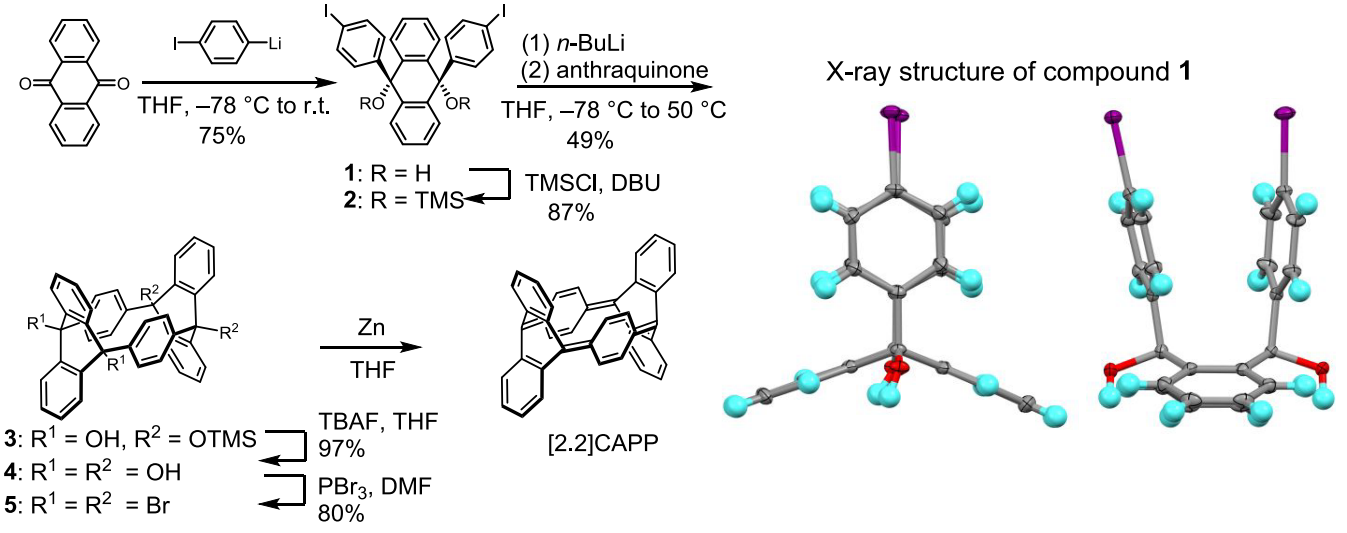

[a]Gray = carbon, blue = hydrogen, red = oxygen, and purple = iodine.

challenges and stability issues.[57−59] In this study, we report the synthesis and properties of [2.2]CAPP. The structural and electronic characteristics of [2.2]CAPP, including its quinoidal nature and optical behavior, are discussed in detail. We also examined the impact of ring strain on the aromaticity and spin

https://doi.org/10.1021/jacs.5c11812
J. Am. Chem. Soc. 2025, 147, 37488−37496

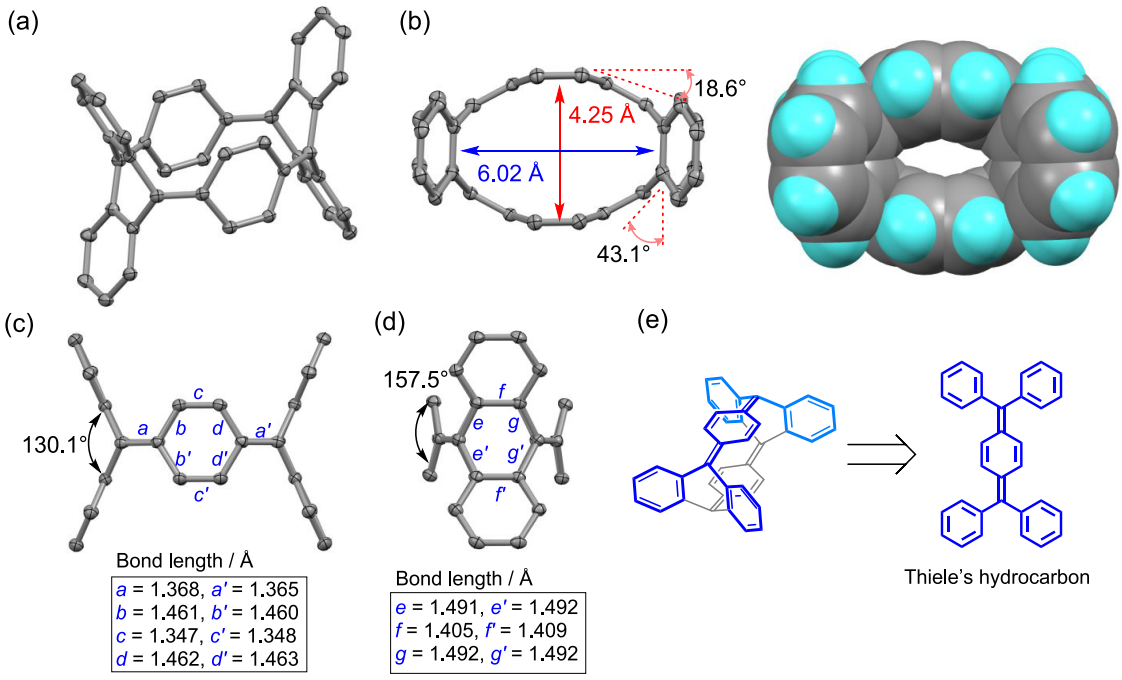

Figure 2. (a) X-ray structure of the [2.2]CAPP. (b) Top view. Ellipsoid model (left) and spacefill model (right). (c) Side view from the phenyl unit. (d) Side view from anthryl unit. Hydrogen atoms are omitted for clarity. (e) Molecular structure of Thiele's hydrocarbon, which is the component of [2.2]CAPP, highlighted by blue.

state of the anthrylene units through X-ray crystallography, NMR spectroscopy, and quantum chemical calculations.

RESULT AND DISCUSSION

Synthesis and Structural Evaluation of [2.2]CAPP. The synthetic route to [2.2]CAPP is outlined in Scheme 1. Starting from anthraquinone, two 4-iodophenyl groups were introduced to afford compound **1**.[60] Notably, single-crystal X-ray analysis of compound **1** revealed that the appended phenyl rings adopt a nearly parallel orientation (Scheme 1 right and Figure S1). This geometry led us to anticipate that the synthesis of [2.2]CAPP would be possible without the use of transition-metal catalysts. Protection of diol **1** with silyl groups gave compound **2**,[61] which underwent dilithiation followed by nucleophilic addition to another equivalent of anthraquinone, affording compound **3** in moderate yield (49%). This compound serves as a key intermediate for the construction of [2.2]CAPP. Subsequent desilylation furnished tetraol **4** in an almost quantitative yield (97%). Attempts to aromatize **4** under typical reductive conditions, such as lithium naphthalide or stannous dichloride, were unsuccessful, resulting instead in partial hydrogenation of the hydroxyl groups. Therefore, compound **4** was converted to the tetrabromo precursor **5** using phosphorus tribromide in a good yield (80%). Final reduction with zinc powder in THF afforded the desired product, [2.2]CAPP. Owing to its high ring strain energy (+88.3 kcal mol^{-1}, estimated by a homodesmotic reaction; Figure S3), [2.2]CAPP was found to be unstable under ambient air and decomposed in solution. Consequently, purification by silica gel column chromatography proved to be difficult. Nevertheless, recrystallization from the reaction mixture under an inert atmosphere successfully yielded single crystals of [2.2]CAPP suitable for X-ray diffraction analysis.

The molecular structure of [2.2]CAPP revealed a distinctly ellipsoidal ring shape, with the anthrylene units bent by 43.1° and the phenylene units bent by 18.6° (Figure 2a,b). The face-to-face distance between the two anthrylene units was 6.02 Å, whereas that between the phenylene units was 4.25 Å, indicating distortion induced by ring strain. The C═C bond lengths between the phenylene and anthrylene units ranged from 1.365 to 1.368 Å, consistent with a quinoidal character. This structural motif differs entirely from the calculated optimized structure of [4]CPP, but closely resembles a cyclic dimer of Thiele's hydrocarbon (Figures 2e and S5). Pronounced bond length alternation (BLA) was observed in the phenylene (0.112−0.115 Å) and anthrylene units (0.083−0.087 Å). In addition, both aromatic units exhibited outwardly curved geometries with bending angles of 130.1° for anthrylene and 157.5° for phenylene. Density functional theory (DFT) calculations well reproduced these structural parameters (Figure S4), and the anthrylene bend angle was comparable to that of the computationally optimized picotube (131.1°) (Figure S5). These results indicate that the high ring strain energy induces a loss of aromatic character in the anthrylene units, promoting the development of open-shell biradical character (Figure 3a).[62] Although higher acenes, such as heptacene and beyond, are known to exhibit open-shell biradical character to gain aromatic stabilization through the formation of additional Clar's aromatic sextets, planar anthracene does not exhibit such biradical character. This is because smaller acenes cannot sufficiently offset the energetic cost of biradical formation with the stabilization provided by an additional Clar's sextet.[63−65] DFT calculations based on the X-ray structure of the bent anthracene core gave a high biradical index (y_0 = 0.89) estimated from the natural orbital occupation number (NOON). Nucleus-independent chemical shift (NICS) calculations for the bent anthracene structure showed that the $NICS(1)_{zz}$ values of the central six-membered ring *a* and *a′* were −0.51 and +6.05 ppm, respectively, indicating a nonaromatic character. This represents a

https://doi.org/10.1021/jacs.5c11812
J. Am. Chem. Soc. 2025, 147, 37488−37496

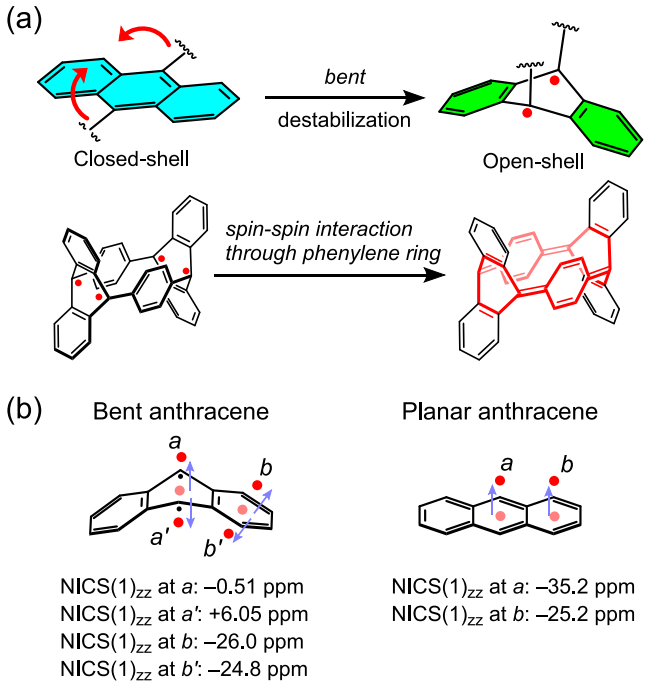

Figure 3. (a) Concept of development of the open-shell nature of the anthrylene unit by strain energy and spin−spin interactions through a phenylene ring to form a quinoidal structure in [2.2]CAPP. (b) NICS $(1)_{zz}$ values of bent and planar anthracenes calculated by the (U)CAM-B3LYP/6−31G**//(U)ωB97X-D/6−31G** level of theory.

significant loss of aromaticity compared to the corresponding value for planar anthracene (−35.2 ppm). In contrast, the terminal six-membered ring *b* and *b′* retained moderate aromatic character, with NICS$(1)_{zz}$ values of −26.0 and −24.8 ppm, respectively (Figure 3b). The calculated singlet−triplet energy gap (ΔE_{S-T}) of the bent anthracene was −0.75 kcal mol^{-1}, which is much smaller than that of planar anthracene (−41.3 kcal mol^{-1}). However, in [2.2]CAPP, the two unpaired electrons on the anthrylene units are stabilized through spin−spin interaction via the phenylene linkers, resulting in an overall closed-shell quinoidal structure. To further evaluate the energetic accessibility of open-shell states, DFT calculations were performed to compare the energies of the closed-shell form with those of open-shell multiradical states, including the triplet and quintet (Figure S4). The calculated energy differences (ΔE_{S-T} and ΔE_{S-Q}) were −38.5 and −44.7 kcal mol^{-1}, respectively, indicating that thermal excitation to these higher spin states is energetically unfavorable. In fact, the ESR measurement of [2.2]CAPP showed no signals from thermally excited species that are characteristic of singlet open-shell compounds (Figure S9), thereby indicating that [2.2]CAPP possesses a closed-shell ground state.

Evaluation of Aromatic Character, Optical Properties, and Reactivity of [2.2] CAPP. To investigate the global aromatic character of the [4]CPP core in [2.2]CAPP, we generated the compound *in situ* in an NMR tube by reacting precursor **5** with zinc powder in THF-d_8. Although several weak peaks attributed to impurities were observed, the signals corresponding to [2.2]CAPP were dominant, indicating that the zinc-mediated reduction of **5** effectively generates [2.2]CAPP (Figure 4a). The ^{1}H NMR spectrum exhibited two AA′XX′ doublet patterns at 7.40 and 7.13 ppm, assigned to the anthrylene protons, and a singlet at 6.54 ppm, attributed to the phenylene unit. The upfield shift of the phenylene resonance, relative to typical aromatic protons as well as those of [5]CPP (7.85 ppm in $CDCl_3$) and [6]CPP (7.63 ppm in $CDCl_3$), is consistent with quinoidal character. Although [2.2]CAPP nominally contains 16π-electrons in the macrocyclic conjugation pathway, suggesting potential antiaromaticity, no evidence for global antiaromatic ring currents was found. The observed chemical shifts are comparable to those of Thiele's hydrocarbon,[66,67] and nucleus-independent chemical shift (NICS) calculations also supported the absence of global antiaromaticity (Figures 4b and S6).

The ultraviolet−visible (UV−vis) absorption and emission spectra of [2.2]CAPP in THF are shown in Figure 5a. Two absorption maxima were observed at 403 and 347 nm. Time-dependent DFT (TD-DFT) calculations revealed that the HOMO → LUMO excitation, corresponding to the $S_0 \rightarrow S_1$ transition, is symmetry-forbidden and appears at 451 nm (f = 0.0000) (Table S3). Compared with the UV−vis absorption spectrum of [5]- and [6]CPPs, that of [2.2]CAPP is entirely different: there is no weak forbidden band at longer wavelength, and the HOMO−LUMO gap is larger, most likely due to the quinoidal character. According to our calculations, the frontier molecular orbitals (FMOs) of [2.2]CAPP more closely resemble those of Thiele's hydro-

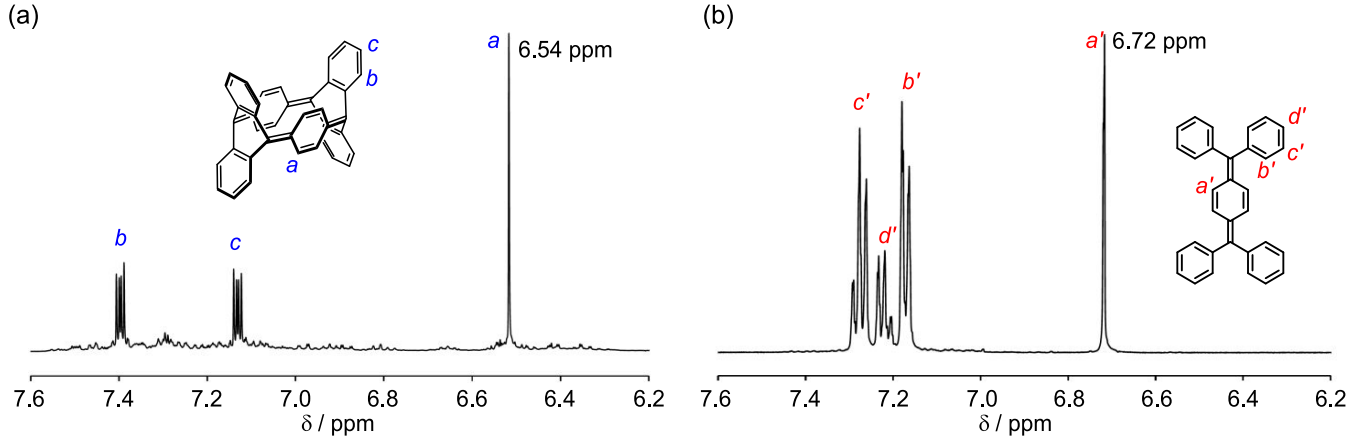

Figure 4. ^{1}H NMR spectrum of (a) [2.2]CAPP and (b) Thiele's hydrocarbon in THF-d_8.

https://doi.org/10.1021/jacs.5c11812
J. Am. Chem. Soc. 2025, 147, 37488−37496

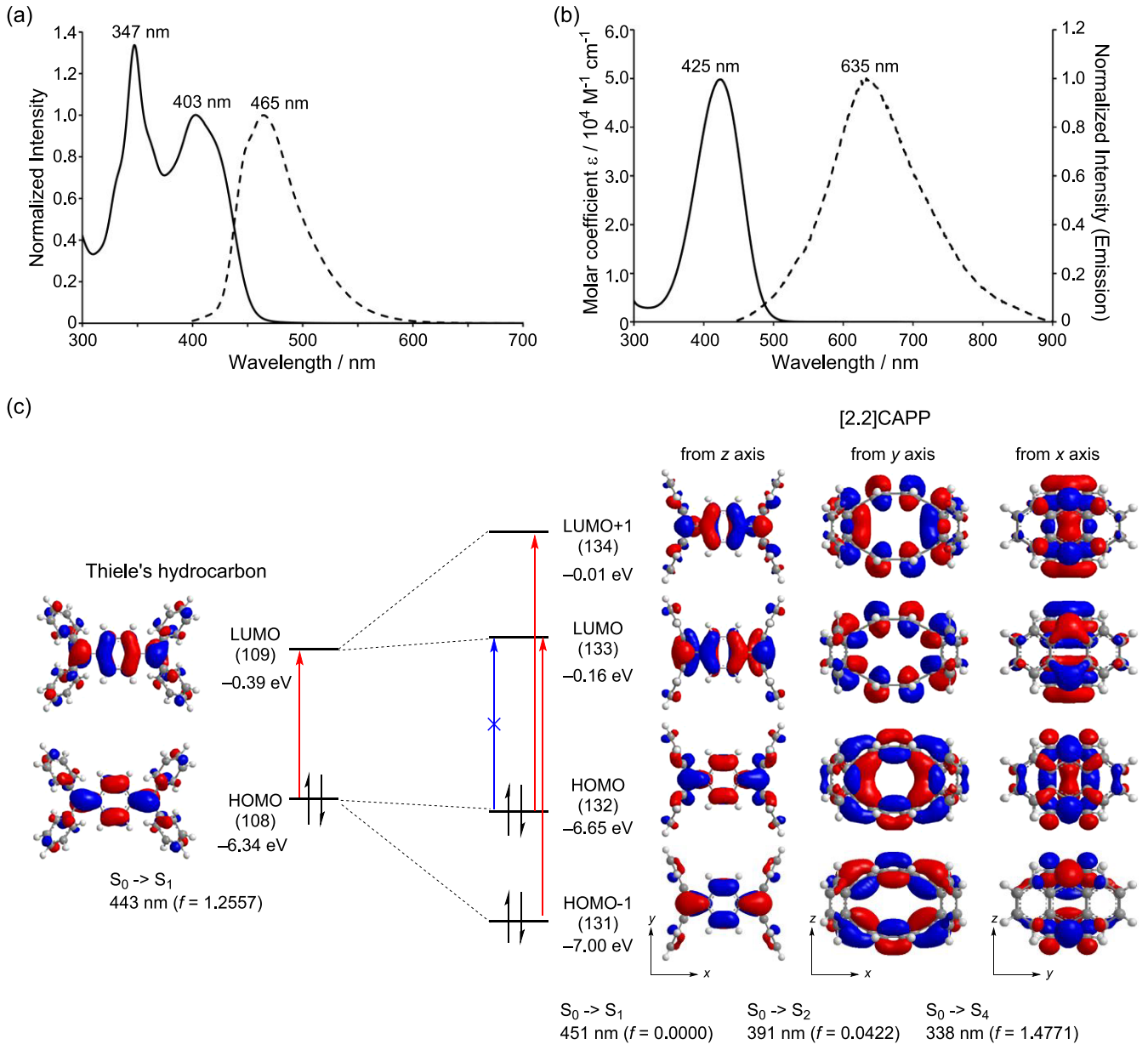

Figure 5. UV−vis and emission spectra of (a) [2.2]CAPP (λ_{ex} = 350 nm) and (b) Thiele's hydrocarbon (λ_{ex} = 400 nm) in THF. (c) Frontier molecular orbitals of Thiele's hydrocarbon (left) and [2.2]CAPP (right) and the results of TD-DFT calculations (CAM-B3LYP/6−311+G**//ωB97X-D/6−31G**).

carbon than those of CPPs (Figure 5c). Interestingly, due to the short face-to-face distance between the *para*-quinodimethane moieties in [2.2]CAPP, it was expected that the HOMO and LUMO orbitals of Thiele's hydrocarbon would split into antibonding (HOMO) and bonding (HOMO−1), and bonding (LUMO) and antibonding (LUMO + 1) orbitals, respectively. However, the FMOs of [2.2]CAPP displayed the opposite trend: bonding orbitals in the HOMO and LUMO+1, and antibonding orbitals in the HOMO−1 and LUMO. Moreover, the HOMO and LUMO energy levels of [2.2]CAPP are quite similar to those of Thiele's hydrocarbon. Further computational investigations revealed that the wave function patterns of these FMOs are essentially identical to those of all-*cis*-[16]annulene (Figure S7), which derives from the cyclic 16π-conjugation in [2.2]CAPP. This indicates that [2.2]CAPP embodies dual electronic features, those of Thiele's hydrocarbon and those of cyclic π-conjugation reminiscent of [16]annulene. As a result, the HOMO → LUMO excitation in [2.2]CAPP corresponds to a transition from a bonding to an antibonding orbital, rendering it symmetry-forbidden. In contrast, the HOMO−1 → LUMO and HOMO → LUMO + 1 excitations corresponding to both $S_0 \rightarrow S_2$ and $S_0 \rightarrow S_4$ transitions are allowed, appearing at 391 nm (f = 0.0422) and 338 nm (f = 1.4471), respectively. This is because the HOMO−1 and LUMO+1 orbitals exhibit antibonding and bonding character, respectively, between the *para*-quinodimethane units, leading to allowed transition pairs. The observed absorption spectrum is similar to, but slightly blue-shifted from, that of Thiele's hydrocarbon (λ_{abs} = 425 nm; Figure 5b).

The reactivity of [2.2]CAPP under air was evaluated by monitoring the decay of its UV−vis spectra. Upon opening the

https://doi.org/10.1021/jacs.5c11812
J. Am. Chem. Soc. 2025, 147, 37488−37496

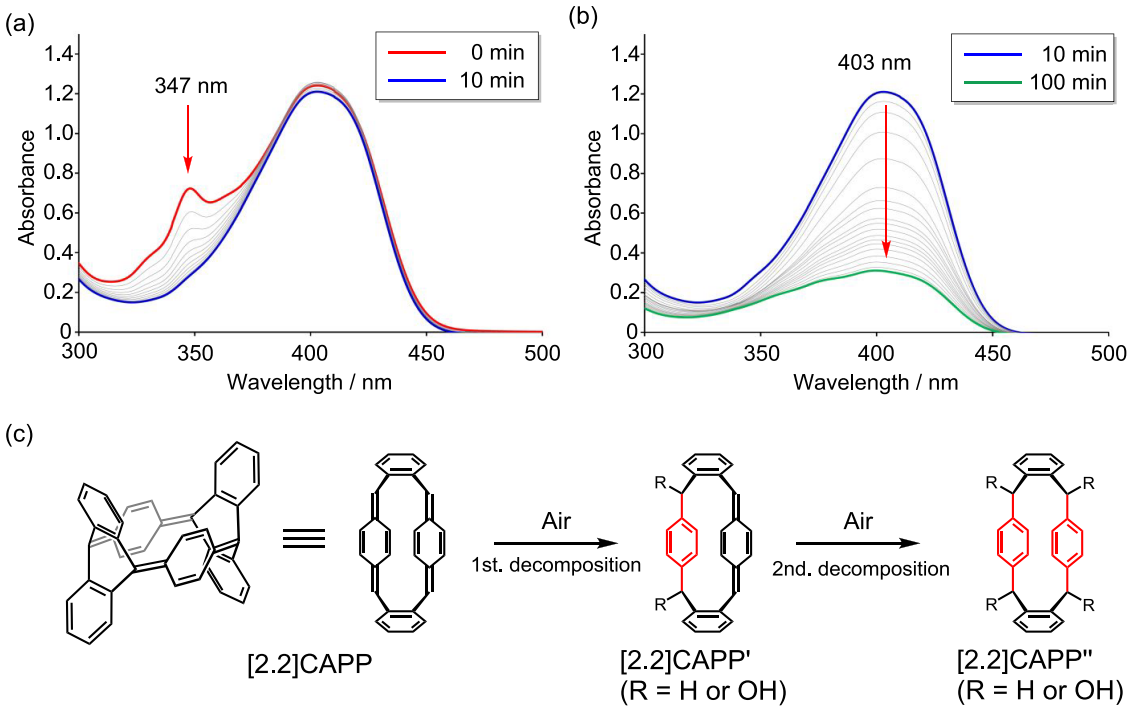

Figure 6. UV−vis absorption decay of [2.2]CAPP after the sealed UV cell. (a) Absorption decay from 0 to 10 min (measured every 1 min). (b) Absorption decay from 10 to 100 min (measured every 5 min). (c) Plausible stepwise decomposition pathway of [2.2]CAPP.

sealed UV cell and exposing the solution to air, the intense peak at 347 nm, corresponding $S_0 \rightarrow S_4$ transition, rapidly disappeared within 10 min (Figure 6a). Remarkably, this high reactivity was observed, despite [2.2]CAPP being a closed-shell molecule. In addition, another intense absorption peak at 403 nm gradually decreased following disappearance of the $S_0 \rightarrow S_4$ transition (Figure 6b). These results indicate that [2.2]CAPP undergoes a two-step decomposition: a rapid initial process with a half-life of *ca.* 2.1 min followed by a slower process with a half-life of *ca.* 43 min (Figure S10), which we attribute to the stepwise degradation of the Thiele subunits, most likely affording [2.2]CAPP′ and [2.2]CAPP″, respectively (Figure 6c). TD-DFT calculations of [2.2]CAPP′ (R = H) show no transition around 350 nm but instead an intense transition at 410 nm (Figure S8 and Table S3), supporting the hypothesis of stepwise decomposition. The second decomposition is significantly faster than that of the pristine Thiele's hydrocarbon ($t_{1/2}$ = 37.3 h, Figure S10), most likely due to the residual ring strain in [2.2]CAPP′.

Notably, [2.2]CAPP exhibits intense emission at 465 nm with a high quantum yield (ϕ_{em} = 82%), even though [5]- and [6]CPPs show no emission owing to very fast nonradiative internal conversion after the excitation caused by their small HOMO−LUMO gaps.[68] In addition, this high quantum emission yield is in stark contrast to the weak emission of Thiele's hydrocarbon (λ_{em} = 635 nm, ϕ_{em} = 0.3%). Thus, this enhanced emission in [2.2]CAPP is likely attributable to the conformational rigidity imposed by the macrocyclic ring, which suppresses nonradiative decay pathways.

Finally, we explored the redox properties of [2.2]CAPP. Given that dicationic forms of [*n*]CPPs often exhibit global aromaticity,[69,70] and computational studies by NICS calculations indicated that the center in macrocycle of [2.2]CAPP with dicationic state shows aromatic character at −17.0 ppm (Figure S6). Although we attempted chemical oxidation using nitrosonium hexafluoroantimonate ($NOSbF_6$), treatment resulted in the formation of insoluble, uncharacterizable material, probably due to the high reactivity arising from the inherent ring strain even under the oxidation state with global aromatic character.

CONCLUSIONS

In summary, we have successfully synthesized [2.2]cyclo(9,10)anthrylene-paraphenylene ([2.2]CAPP), a [4]CPP-type macrocycle composed of alternating anthrylene and phenylene units. This compound was prepared in six steps from commercially available anthraquinone without the use of transition-metal-catalyzed coupling reactions. Single-crystal X-ray diffraction analysis confirmed the formation of a quinoidal structure with bent anthrylene units, indicative of aromatic destabilization caused by high ring strain. ^{1}H NMR spectroscopy revealed that the phenylene protons appeared at a relatively high field, consistent with a quinoidal electronic structure and the absence of global antiaromaticity. Optical characterization demonstrated intense emission with a high quantum yield, which was attributed to conformational rigidity within the macrocycle. These findings indicate that a high ring strain can effectively suppress aromaticity in anthrylene units and promote open-shell character. The interaction of unpaired electrons through phenylene linkers facilitates the formation of a closed-shell quinoidal structure, but the high reactivity toward air is retained. Thus, [2.2]CAPP can be viewed as a cyclic dimer of Thiele's hydrocarbon. This strategy highlights a new approach to constructing open-shell carbon nanorings composed entirely of six-membered rings. Future work will focus on tuning the electronic properties by modifying the spacer units and expanding the family of strained open-shell carbon nanorings.

https://doi.org/10.1021/jacs.5c11812
J. Am. Chem. Soc. 2025, 147, 37488−37496

■ ASSOCIATED CONTENT

Supporting Information

The Supporting Information is available free of charge at https://pubs.acs.org/doi/10.1021/jacs.5c11812.

Full synthetic; crystallographic; and computational details as well as spectroscopic data for new compounds (PDF)

Accession Codes

Deposition Numbers 2464521−2464522 contain the supplementary crystallographic data for this paper. These data can be obtained free of charge via the joint Cambridge Crystallographic Data Centre (CCDC) and Fachinformationszentrum Karlsruhe Access Structures service.

■ AUTHOR INFORMATION

Corresponding Author

Tomohiko Nishiuchi − *Department of Chemistry, Graduate School of Science, The University of Osaka, Osaka 560-0043, Japan; Innovative Catalysis Science Division, Institute for Open and Transdisciplinary Research Initiatives, (ICS-OTRI), The University of Osaka, Osaka 565-0871, Japan;* orcid.org/0000-0002-2113-0731; Email: nishiuchit13@chem.sci.osaka-u.ac.jp

Authors

Yuta Makihara − *Department of Chemistry, Graduate School of Science, The University of Osaka, Osaka 560-0043, Japan*

Takashi Kubo − *Department of Chemistry, Graduate School of Science, The University of Osaka, Osaka 560-0043, Japan; Innovative Catalysis Science Division, Institute for Open and Transdisciplinary Research Initiatives, (ICS-OTRI) and Spintronics Research Network Division, Institute for Open and Transdisciplinary Research Initiatives (SPIN-OTRI), The University of Osaka, Osaka 565-0871, Japan;* orcid.org/0000-0001-6809-7396

Complete contact information is available at: https://pubs.acs.org/10.1021/jacs.5c11812

Author Contributions

All authors have given approval to the final version of the manuscript.

Notes

The authors declare no competing financial interest.

■ ACKNOWLEDGMENTS

This study was supported by Grant-in-Aid for Scientific Research (B) (JSPS KAKENHI grant no. JP24K01454, T.N.) and in part by Scientific Research (A) (JSPS KAKENHI grant no. JP24H00459, T.K.). Quantum chemical calculations were performed at the Research Center for Computational Science, Okazaki, Japan (Project: 24-IMS-C214 and 25-IMS-C291). This work was the result of using research equipment shared in the MEXT Project for promoting public utilization of advanced research infrastructure (Program for Supporting Construction of Core Facilities, grant no. JPMXS0441200024).

■ REFERENCES

(1) Heilbronner, E. Molecular Orbitals in homologen Reihen mehrkerniger aromatischer Kohlenwasserstoffe: I. Die Eigenwerte yon LCAO-MO's in homologen Reihen. *Helv. Chim. Acta* **1954**, *37*, 921−935.

(2) Aihara, J.-i. Aromaticity and Superaromaticity in Cyclopolyacenes. *J. Chem. Soc., Perkin Trans. 2* **1994**, *2*, 971−974.

(3) Choi, H. S.; Kim, K. S. Structures, Magnetic Properties, and Aromaticity of Cyclacenes. *Angew. Chem., Int. Ed.* **1999**, *38*, 2256−2258.

(4) Houk, K. N.; Lee, P. S.; Nendel, M. Polyacene and Cyclacene Geometries and Electronic Structures: Bond Equalization, Vanishing Band Gaps, and Triplet Ground States Contrast with Polyacetylene. *J. Org. Chem.* **2001**, *66*, 5517−5521.

(5) Türker, L.; Gümüş, S. Cyclacenes. *J. Mol. Struct. Theochem* **2004**, *685*, 1−33.

(6) Chen, Z.; Jiang, D.-e.; Lu, X.; Bettinger, H. F.; Dai, S.; Schleyer, P. v. R.; Houk, K. N. Open-Shell Singlet Character of Cyclacenes and Short Zigzag Nanotubes. *Org. Lett.* **2007**, *9*, 5449−5452.

(7) Somani, A.; Gupta, D.; Bettinger, H. F. Computational Studies of Dimerization of [*n*]-Cyclacenes. *J. Phys. Chem. A* **2024**, *128*, 6847−6852.

(8) Vögtle, F.; Cyclophanes, I. I. Concluding remarks. *Top. Curr. Chem.* **1983**, *115*, 157−159.

(9) Kohnke, F. H.; Slawin, A. M. Z.; Stoddart, J. F.; Williams, D. J. Molecular Belts and Collars in the Making: A Hexaepoxyoctacosahydro[12]cyclacene Derivative. *Angew. Chem., Int. Ed.* **1987**, *26*, 892−894.

(10) Ashton, P. R.; Isaacs, N. S.; Kohnke, F. H.; Slawin, A. M. Z.; Spencer, C. M.; Stoddart, J. F.; Williams, D. J. Towards the Making of [12]Collarene. *Angew. Chem., Int. Ed.* **1988**, *27*, 966−969.

(11) Cory, R. M.; McPhail, C. L. Fascinating Stops on the Way to Cyclacenes and Cyclacene Quinones: A tour guide to synthetic progress to date. In *Advances in Theoretically Interesting Molecules*; Thummel, R. P., Ed.; JAI Press, 1998; Vol. *4*, pp 53−80.

(12) Godt, A.; Enkelmann, V.; Schlüter, A. D. Double-stranded molecules: a [6]beltene derivative and the corresponding open-chain polymer. *Angew. Chem., Int. Ed.* **1989**, *28*, 1680−1682.

(13) Vögtle, F.; Schröder, A.; Karbach, D. Strategy for the synthesis of tube-shaped molecules. *Angew. Chem., Int. Ed.* **1991**, *30*, 575−577.

(14) Kawase, T.; Darabi, H. R.; Oda, M. Cyclic [6]- and [8]paraphenylacetylenes. *Angew. Chem., Int. Ed.* **1996**, *35*, 2664−2666.

(15) Nakamura, E.; Tahara, K.; Matsuo, Y.; Sawamura, M. Synthesis, Structure, and Aromaticity of a Hoop-Shaped Cyclic Benzenoid [10]Cyclophenacene. *J. Am. Chem. Soc.* **2003**, *125*, 2834−2835.

(16) Scott, L. T. Conjugated belts and nanorings with radially oriented *p* orbitals. *Angew. Chem., Int. Ed.* **2003**, *42*, 4133−4135.

(17) Hellbach, B.; Rominger, F.; Gleiter, R. Synthesis of Beltenes by Reactions of 5,6,11,12-Tetradehydrodibenzo[a,e]cyclooctene with [$CpCo(CO)_2$] Derivatives. *Angew. Chem., Int. Ed.* **2004**, *43*, 5846−5849.

(18) Tahara, K.; Tobe, Y. Molecular Loops and Belts. *Chem. Rev.* **2006**, *106*, 5274−5290.

(19) Kawase, T.; Kurata, H. Ball-, Bowl-, and Belt-Shaped Conjugated Systems and Their Complexing Abilities: Exploration of the Concave-Convex π-π Interaction. *Chem. Rev.* **2006**, *106*, 5250−5273.

(20) Esser, B.; Rominger, F.; Gleiter, R. Synthesis of $[6.8]_3$Cyclacene: Conjugated Belt and Model for an Unusual Type of Carbon Nanotube. *J. Am. Chem. Soc.* **2008**, *130*, 6716−6717.

(21) Jasti, R.; Bhattacharjee, J.; Neaton, J. B.; Bertozzi, C. R. Synthesis, Characterization, and Theory of [9]-, [12]-, and [18]-Cycloparaphenylene: Carbon Nanohoop Structures. *J. Am. Chem. Soc.* **2008**, *130*, 17646−17647.

(22) Takaba, H.; Omachi, H.; Yamamoto, Y.; Bouffard, J.; Itami, K. Selective Synthesis of [12]Cycloparaphenylene. *Angew. Chem., Int. Ed.* **2009**, *48*, 6112−6116.

(23) Gleiter, R.; Esser, B.; Kornmayer, S. C. Cyclacenes: Hoop-shaped systems composed of conjugated rings. *Acc. Chem. Res.* **2009**, *42*, 1108−1116.

(24) Yamago, S.; Watanabe, Y.; Iwamoto, T. Synthesis of [8]Cycloparaphenylene from a Square-Shaped Tetranuclear Platinum Complex. *Angew. Chem., Int. Ed.* **2010**, *49*, 757−759.

(25) Eisenberg, D.; Shhenhar, R.; Rabinovitz, M. Synthetic approaches to aromatic belts: building up strain in macrocyclic polyarenes. *Chem. Soc. Rev.* **2010**, *39*, 2879−2890.
(26) Hitosugi, S.; Nakanishi, W.; Yamasaki, T.; Isobe, H. Bottom-up synthesis of finite models of helical (*n*,*m*)-single-wall carbon nanotubes. *Nat. Commun.* **2011**, *2*, No. 492.
(27) Iyoda, M.; Kuwatani, Y.; Nishinaga, T.; Takase, M.; Nishiuchi, T. Conjugated molecular belts based on 3D benzannulene systems. In *Fragments of Fullerenes and Carbon Nanotubes*; Petrukhina, M. A.; Scott, L. T., Eds.; Wiley, 2011.
(28) Schaller, G. R.; Herges, R. Aromatic belts as sections of nanotubes. In *Fragments of Fullerenes and Carbon Nanotubes*; Petrukhina, M. A.; Scott, L.T., Eds.; Wiley, 2011.
(29) Nishiuchi, T.; Feng, X.; Enkelmann, V.; Wagner, M.; Müllen, K. Three-Dimensionally Arranged Cyclic p-Hexaphenylbenzene: Toward a Bottom-Up Synthesis of Size-Defined Carbon Nanotubes. *Chem. - Eur. J.* **2012**, *18*, 16621−16625.
(30) Yagi, A.; Segawa, Y.; Itami, K. Synthesis and Properties of [9]Cyclo-1,4-naphthylene: A π-Extended Carbon Nanoring. *J. Am. Chem. Soc.* **2012**, *134*, 2962−2965.
(31) Matsuno, T.; Kamata, S.; Hitosugi, S.; Isobe, H. Bottom-up synthesis and structures of π-lengthened tubular macrocycles. *Chem. Sci.* **2013**, *4*, 3179−3183.
(32) Yamago, S.; Kayahara, E.; Iwamoto, T. Organoplatinum-Mediated Synthesis of Cyclic π-Conjugated Molecules: Towards a New Era of Three-Dimensional Aromatic Compounds. *Chem. Rec.* **2014**, *14*, 84−100.
(33) Golling, F. E.; Quernheim, M.; Wagner, M.; Nishiuchi, T.; Müllen, K. Concise synthesis of 3D π-extended polyphenylene cylinders. *Angew. Chem., Int. Ed.* **2014**, *53*, 1525−1528.
(34) Iwamoto, T.; Kayahara, E.; Yasuda, N.; Suzuki, T.; Yamago, S. Synthesis, characterization, and properties of [4]cyclo-2,7-pyrenylene: Effects of cyclic structure on the electronic properties of pyrene oligomers. *Angew. Chem., Int. Ed.* **2014**, *53*, 6430−6434.
(35) Golder, M. R.; Jasti, R. Syntheses of the Smallest Carbon Nanohoops and the Emergence of Unique Physical Phenomena. *Acc. Chem. Res.* **2015**, *48*, 557−566.
(36) Povie, G.; Segawa, Y.; Nishihara, T.; Miyauchi, Y.; Itami, K. Synthesis of a carbon nanobelt. *Science* **2017**, *356*, 172−175.
(37) Cheung, K. Y.; Gui, S.; Deng, C.; Liang, H.; Xia, Z.; Liu, Z.; Chi, L.; Miao, Q. Synthesis of armchair and chiral carbon nanobelts. *Chem* **2019**, *5*, 838−847.
(38) Tsuchido, Y.; Abe, R.; Ide, T.; Osakada, K. A Macrocyclic Gold(I)−Biphenylene Complex: Triangular Molecular Structure with Twisted Au_2(diphosphine) Corners and Reductive Elimination of [6]Cycloparaphenylene. *Angew. Chem., Int. Ed.* **2020**, *59*, 22928−22932.
(39) Guo, Q.-H.; Qiu, Y.; Wang, M.-X.; Stoddart, J. F. Aromatic hydrocarbon belts. *Nat. Chem.* **2021**, *13*, 402−419.
(40) Cheung, K. Y.; Watanabe, K.; Segawa, Y.; Itami, K. Synthesis of a zigzag carbon nanobelt. *Nat. Chem.* **2021**, *13*, 255−259.
(41) Han, Y.; Dong, S.; Shao, J.; Fan, W.; Chi, C. Synthesis of a sidewall fragment of a (12,0) carbon nanotube. *Angew. Chem., Int. Ed.* **2021**, *60*, 2658−2662.
(42) Wössner, J. S.; Wassy, D.; Weber, A.; Bovenkerk, M.; Hermann, M.; Schmidt, M.; Esser, B. *n*]Cyclodibenzopentalenes as Antiaromatic Curved Nanocarbons with High Strain and Strong Fullerene Binding. *J. Am. Chem. Soc.* **2021**, *143*, 12244−12252.
(43) Segawa, Y.; Watanabe, T.; Yamanoue, K.; Kuwayama, M.; Watanabe, K.; Pirillo, J.; Hijikata, Y.; Itami, K. Synthesis of a Möbius carbon nanobelt. *Nat. Synth.* **2022**, *1*, 535−541.
(44) Imoto, D.; Yagi, A.; Itami, K. Carbon Nanobelts: Brief History and Perspective. *Precis. Chem.* **2023**, *1*, 516−523.
(45) Fan, W.; Fukunaga, T. M.; Wu, S.; Han, Y.; Zhou, Q.; Wang, J.; Li, Z.; Hou, X.; Wei, H.; Ni, Y.; Isobe, H.; Wu, J. Synthesis and chiral resolution of a triply twisted Möbius carbon nanobelt. *Nat. Synth.* **2023**, *2*, 880−887.
(46) Han, Y.; Wu, S.; Khoo, K. Y. S.; Chi, C. Synthesis of fully π-conjugated non-alternant carbon nanobelts. *Nat. Synth.* **2025**, *4*, 947−955.
(47) Iwamoto, T.; Watanabe, Y.; Sakamoto, Y.; Suzuki, T.; Yamago, S. Selective and Random Syntheses of [*n*]Cycloparaphenylenes (*n* = 8−13) and Size Dependence of Their Electronic Properties. *J. Am. Chem. Soc.* **2011**, *133*, 8354−8361.
(48) Bachrach, S. M.; Stück, D. DFT Study of Cycloparaphenylenes and Heteroatom-Substituted Nanohoops. *J. Org. Chem.* **2010**, *75*, 6595−6604.
(49) Kayahara, E.; Patel, V. K.; Yamago, S. Synthesis and Characterization of [5]Cycloparaphenylene. *J. Am. Chem. Soc.* **2014**, *136*, 2284−2287.
(50) Evans, P. J.; Darzi, E. R.; Jasti, R. Efficient room-temperature synthesis of a highly strained carbon nanohoop fragment of buckminsterfullerene. *Nat. Chem.* **2014**, *6*, 404−408.
(51) The generation of the smallest CPP derivative, a substituted [2]CPP, was reported. Tsuji, T.; Okuyama, M.; Ohkita, M.; Imai, T.; Suzuki, T. Tricyclo[4.2.2.$2^{2,5}$]dodeca-1,3,5,7,9,11-hexaene: generation and chemical trapping of the 3,4-dicyano derivative. *Chem. Commun.* **1997**, 2151−2152.
(52) Tetrabenzo[2]CPP was reported. Viavattene, R. L.; Greene, F. D.; Cheung, L. D.; Majeste, R.; Trefonas, L. M. 9,9′,10,10′-Tetradehydrodianthracene. Formation, protection, and regeneration of a strained double bond. *J. Am. Chem. Soc.* **1974**, *96*, 4342−4343.
(53) Kammermeier, S.; Jones, P. G.; Herges, R. Ring-Expanding Metathesis of Tetradehydro-anthracene−Synthesis and Structure of a Tubelike, Fully Conjugated Hydrocarbon. *Angew. Chem., Int. Ed.* **1996**, *35*, 2669−2671.
(54) Herges, R.; Deichmann, M.; Grunenberg, J.; Bucher, G. A highly correlated conformational motion of a tube-like fully conjugated hydrocarbon. *Chem. Phys. Lett.* **2000**, *327*, 149−152.
(55) Treitel, N.; Deichmann, M.; Sternfeld, T.; Sheradsky, T.; Herges, R.; Rabinovitz, M. Picotube Tetraanion: A Novel Lithiated Tubular System. *Angew. Chem., Int. Ed.* **2003**, *42*, 1172−1176.
(56) Bhattacharjee, R.; Tovar, J. D.; Kertesz, M. Quinonoid radial π-conjugation. *Chem. Sci.* **2025**, *16*, 14595−14604.
(57) Sun, Z.; Miyamoto, N.; Sato, S.; Tokuyama, H.; Isobe, H. An Obtuse-angled Corner Unit for Fluctuating Carbon Nanohoops. *Chem. Asian J.* **2017**, *12*, 271−275.
(58) Sala, P. D.; Capobianco, A.; Caruso, T.; Talotta, C.; De Rosa, M.; Neri, P.; Peluso, A.; Gaeta, C. An Anthracene-Incorporated [8]Cycloparaphenylene Derivative as an Emitter in Photon Upconversion. *J. Org. Chem.* **2018**, *83*, 220−227.
(59) Xu, Y.; Gsänger, S.; Minameyer, M. B.; Imaz, I.; Maspoch, D.; Shyshov, O.; Schwer, F.; Ribas, X.; Drewello, T.; Meyer, B.; Delius, M. Highly Strained, Radially π-Conjugated Porphyrinylene Nanohoops. *J. Am. Chem. Soc.* **2019**, *141*, 18500−18507.
(60) Csoregh, I.; Brehmer, T.; Bombicz, P.; Weber, E. Halogen···halogen versus OH···O supramolecular interactions in the crystal structures of a series of halogen and methyl substituted *cis*-9,10-diphenyl-9,10-dihydroanthracene-9,10-diols. *Cryst. Eng.* **2001**, *4*, 343−357.
(61) Patel, V. K.; Kayahara, E.; Yamago, S. Practical Synthesis of [*n*]Cycloparaphenylenes (*n* = 5, 7−12) by H_2SnCl_4-Mediated Aromatization of 1,4-Dihydroxycyclo-2,5-diene Precursors. *Chem. − Eur. J.* **2015**, *21*, 5742−5749.
(62) A highly bent anthracene derivative that nevertheless retains a closed-shell electronic structure was reported. Tobe, Y.; Ishii, H.; Saiki, S.; Kakiuchi, K.; Naemura, K. Synthesis and Molecular Structure of 1,4,5,8-Tetramethyl[6](9,10)anthracenophane: The Smallest 9,10-Bridged Anthracene. *J. Am. Chem. Soc.* **1993**, *115*, 11604−11605.
(63) Randić, M. Aromaticity of Polycyclic Conjugated Hydrocarbons. *Chem. Rev.* **2003**, *103*, 3449−3606.
(64) Watanabe, M.; Chen, K.-Y.; Chang, Y. J.; Chow, T. J. Acenes Generated from Precursors and Their Semiconducting Properties. *Acc. Chem. Res.* **2013**, *46*, 1606−1615.

https://doi.org/10.1021/jacs.5c11812
J. Am. Chem. Soc. 2025, 147, 37488−37496

(65) Lerena, L.; Zuzak, R.; Godlewski, S.; Echavarren, A. M. The Journey for the Synthesis of Large Acenes. *Chem. – Eur. J.* **2024**, *30*, No. e202402122.
(66) Thiele, J.; Balhorn, H. Ueber einen chinoïden Kohlenwasserstoff. *Ber. Dtsch. Chem. Ges.* **1904**, *37*, 1463–1470.
(67) Montgomery, L. K.; Huffman, J. C.; Jurczak, E. A.; Grendze, M. P. The molecular structures of Thiele's and Chichibabin's hydrocarbons. *J. Am. Chem. Soc.* **1986**, *108*, 6004–6011.
(68) Fujitsuka, M.; Lu, C.; Zhuang, B.; Kayahara, E.; Kayahara, E.; Yamago, S.; Yamago, S.; Majima, T. Size-Dependent Relaxation Processes of Photoexcited [*n*]Cycloparaphenylenes (*n* = 5–12): Significant Contribution of Internal Conversion in Smaller Rings. *J. Phys. Chem. A* **2019**, *123*, 4737–4742.
(69) Toriumi, N.; Muranaka, A.; Kayahara, E.; Yamago, S.; Uchiyama, M. In-Plane Aromaticity in Cycloparaphenylene Dications: A Magnetic Circular Dichroism and Theoretical Study. *J. Am. Chem. Soc.* **2015**, *137*, 82–85.
(70) Kayahara, E.; Kouyama, T.; Kato, T.; Yamago. Synthesis and Characterization of [*n*]CPP (*n* = 5, 6, 8, 10, and 12) Radical Cation and Dications: Size-Dependent Absorption, Spin, and Charge Delocalization. *J. Am. Chem. Soc.* **2016**, *138*, 338–344.

https://doi.org/10.1021/jacs.5c11812
J. Am. Chem. Soc. 2025, 147, 37488–37496